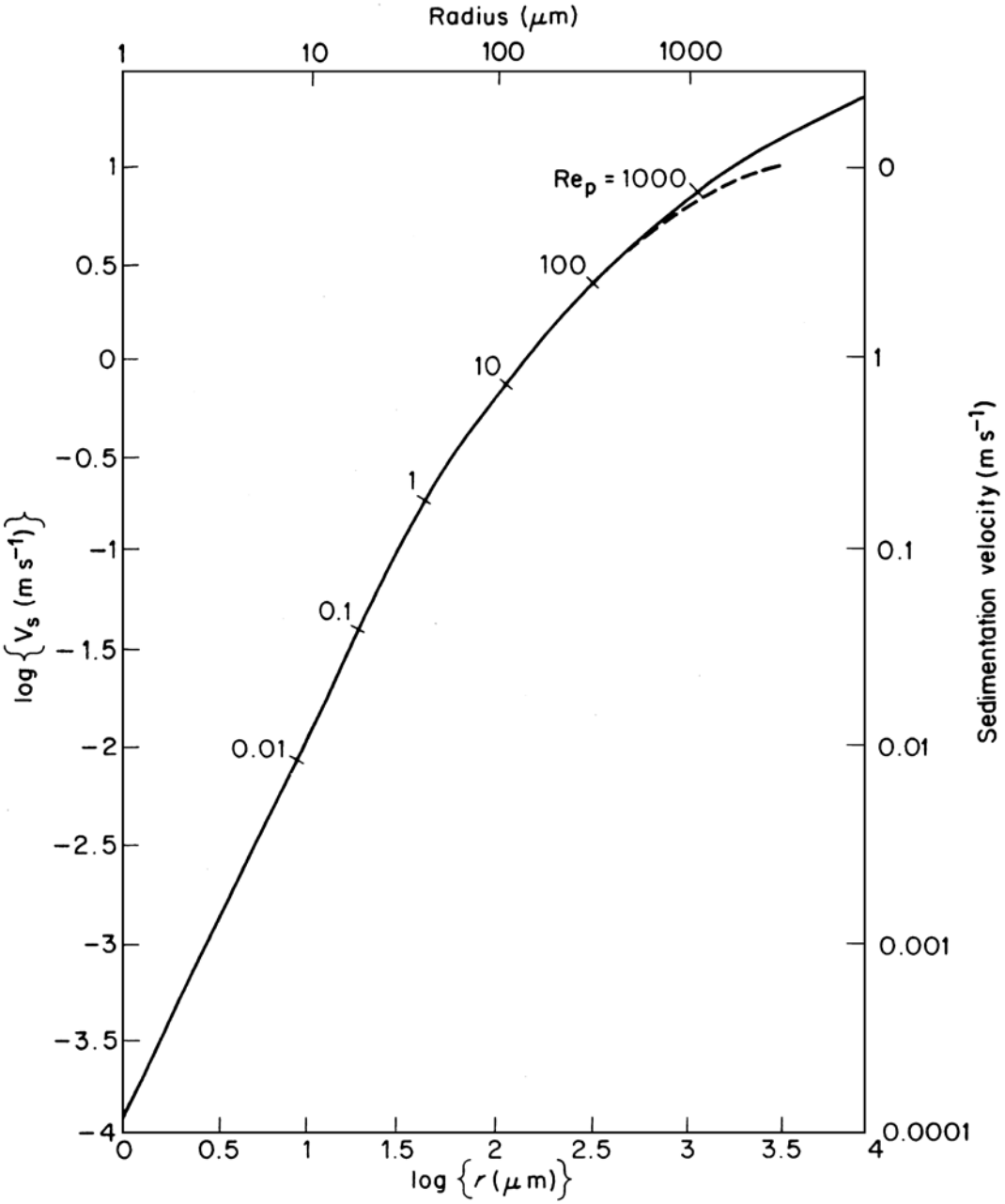

Figure 12.1 Dependence of sedimentation velocity on particle radius for spherical particles with density 1 g cm^{-3}. Stokes' Law applies for $Re_p < 0.1$.
The pecked line shows the sedimentation velocity of raindrops, which is less than that of spheres of equivalent diameter because large raindrops lose their spherical shape as they fall (from Fuchs, 1964). For more detail see http://pmm.nasa.gov/node/145

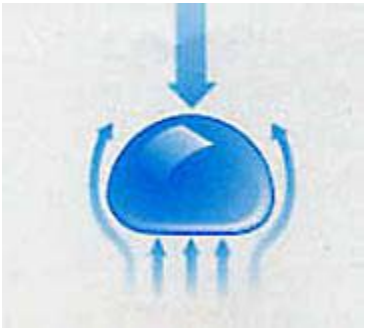

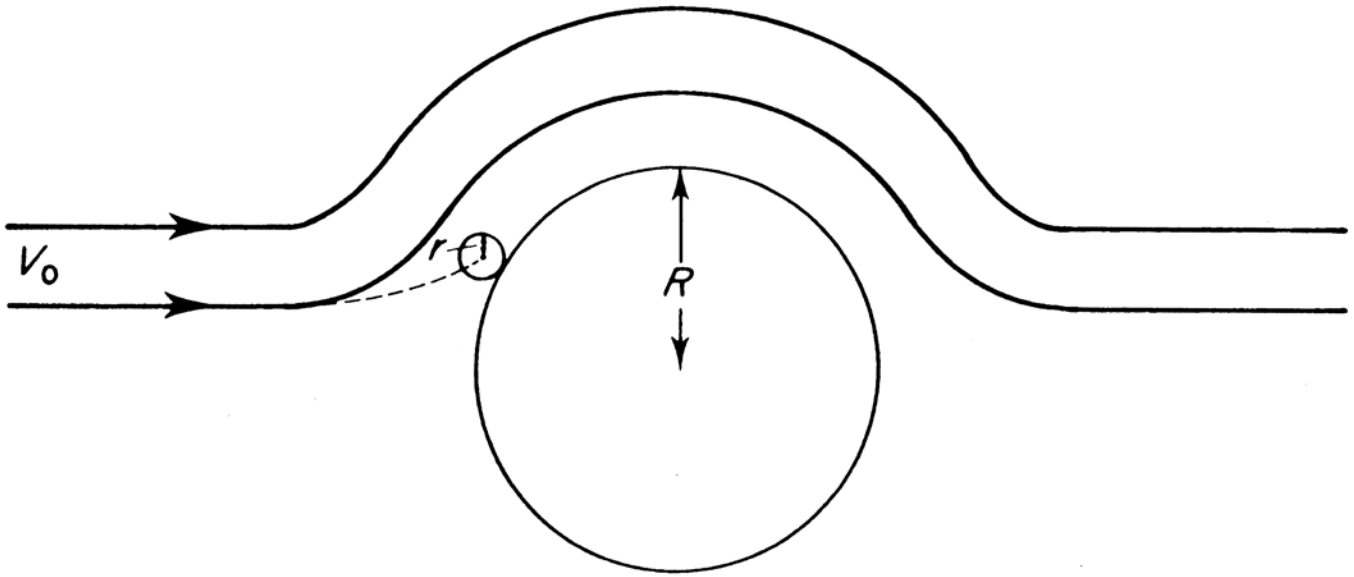

Figure 12.2 Impaction of a particle on a cylinder.

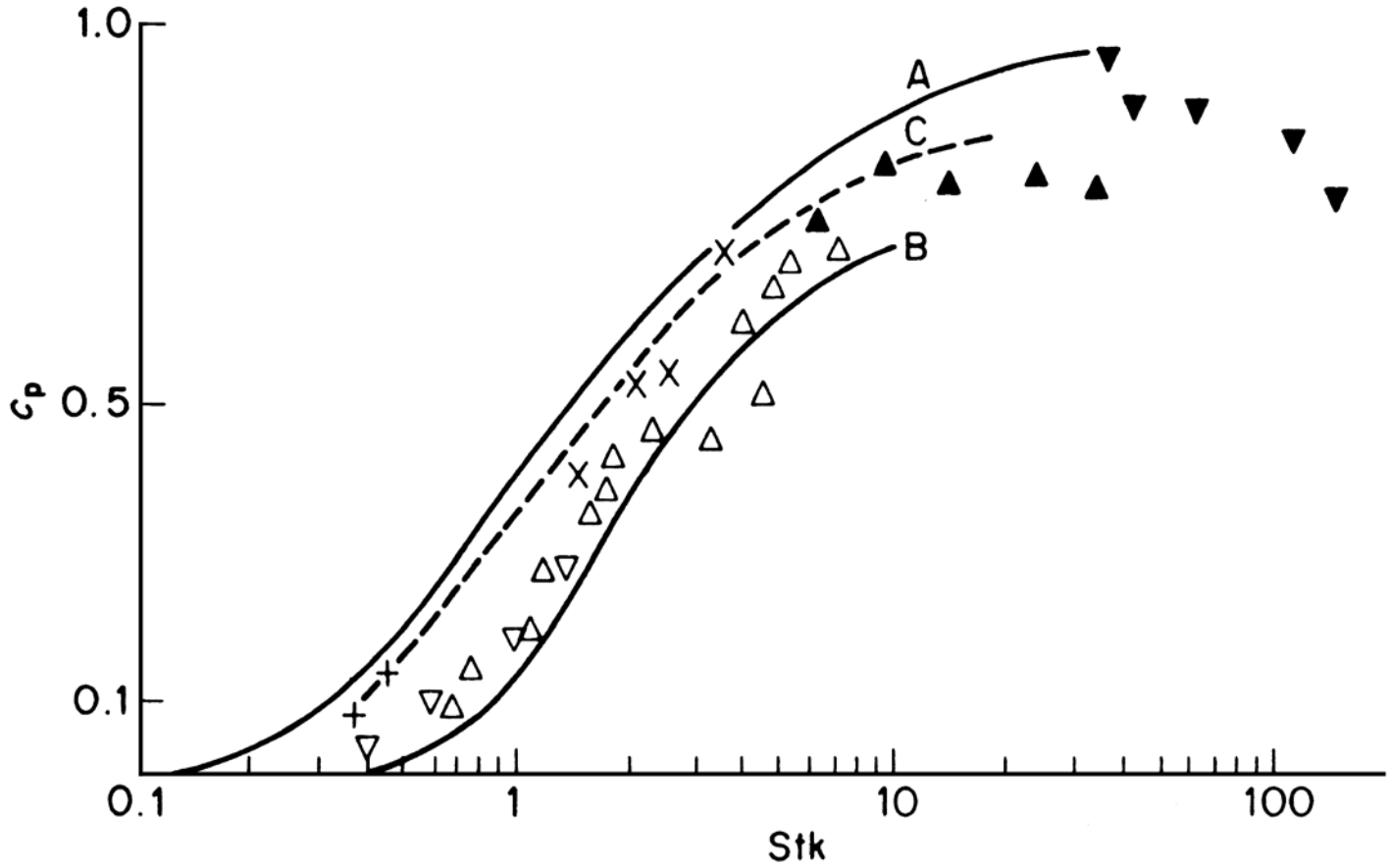

Figure 12.3 Efficiency of impaction of particles (radius *r*) on cylinders (radius *R*) (from Chamberlain, 1975): A and B are theoretical relationships for flow Reynolds numbers Re > 100 and Re = 10, respectively. Line C is fitted to experimental measurements with droplets. The plotted points are measurements with spores impacting on sticky cylinders as follows:

Symbol	+	×	▽	△	▲	▼
r (μm)	2.3	6.4	15	15	15	15
R (mm)	0.1–0.8	0.1–0.8	10	3.3	0.4	0.09

Figure 12.4 (a) Drops of fog which have impacted on and been intercepted by threads of a spider's web. The threads of the web are at least an order of magnitude smaller than individual drops (typically 10−20 μm diameter) and so are efficient collectors by interception (p. 204).

Fig 12.4(b) Drops of fog collected on an author's beard after cycling. Human hair is about 50 µm diameter and cloud drops are about 10 µm diameter, so the drops visible in this picture must have coalesced from many impacted fog drops.

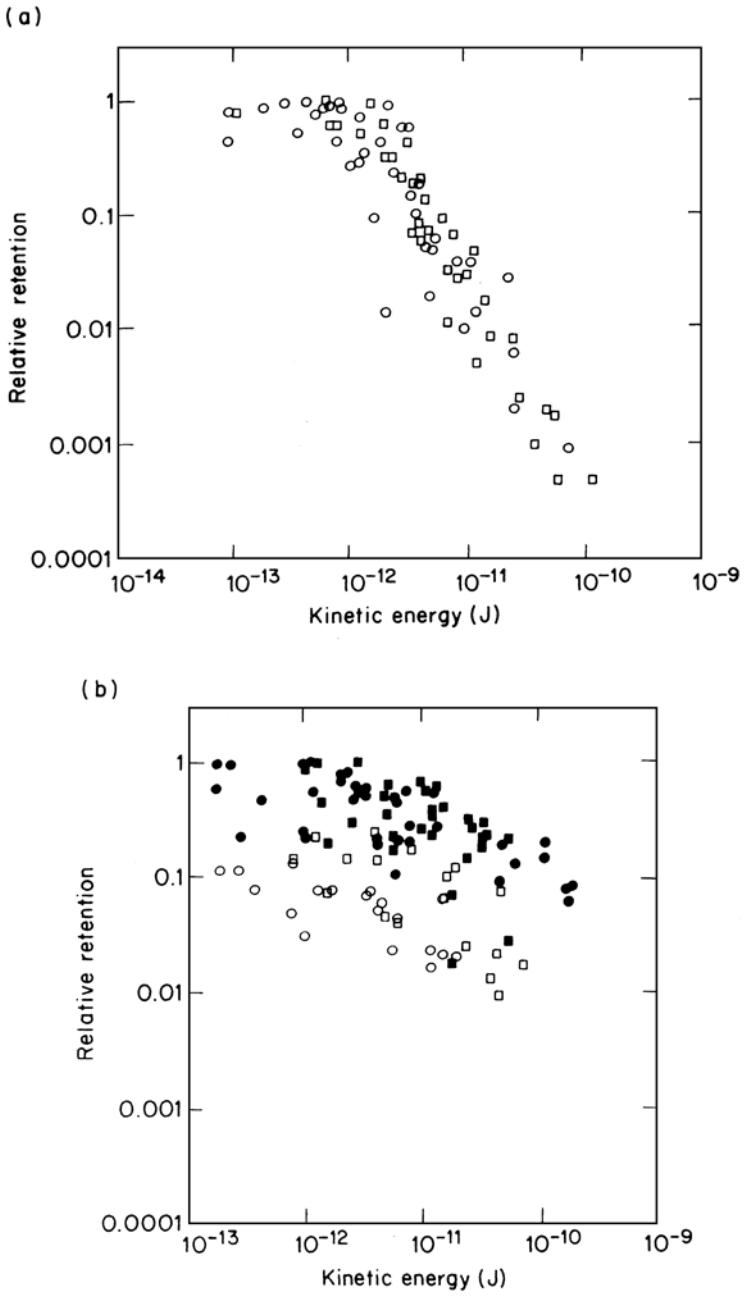

Figure 12.5 Variation with kinetic energy at impact of the relative retention for ragweed (○) and *Lycopodium* (□) particles impacting (a) on glass rods, diameters 3, 5, and 10 mm, in a wind tunnel, and (b) on wheat stems 3–4 mm diameter in the wind tunnel (filled symbols) or in the field (open symbols). (From Aylor and Ferrandino, 1985)

Table 12.1 Deposition of Particles on Segments of Real Leaves, and on Filter Paper, as a Proportion of Deposition on Sticky Artificial Leaves made of PVC (from Chamberlain, 1975)

Particle	Relative deposition					
	Diameter (μm)	Grass	Plantain	Clover	Filter paper	Sticky pvc
Lycopodium spore	32	0.45	0.26	0.18	0.70	1.00
Ragweed pollen	19	0.15	0.11	0.23	0.68	1.00
Polystyrene	5	1.74	1.82	3.25	1.98	1.00
Tricresylphosphate	1	1.70	2.60	5.50	6.40	1.00
Aitken nuclei	0.08	1.06	1.70	0.86	1.54	1.00

Table 12.2 Characteristic Distances for Particle Transport

Particle Radius r (μm)	**0.01**	**0.1**	**1**	**10**
Stopping distance (μm) given initial velocity of 1 m s^{-1}	14×10^{-3}	0.23	13	1230
Distance (μm) traveled in 1 s by virtue of:				
Terminal velocity	14×10^{-2}	2.2	128	1200
Brownian diffusion	160	21	5	1.5

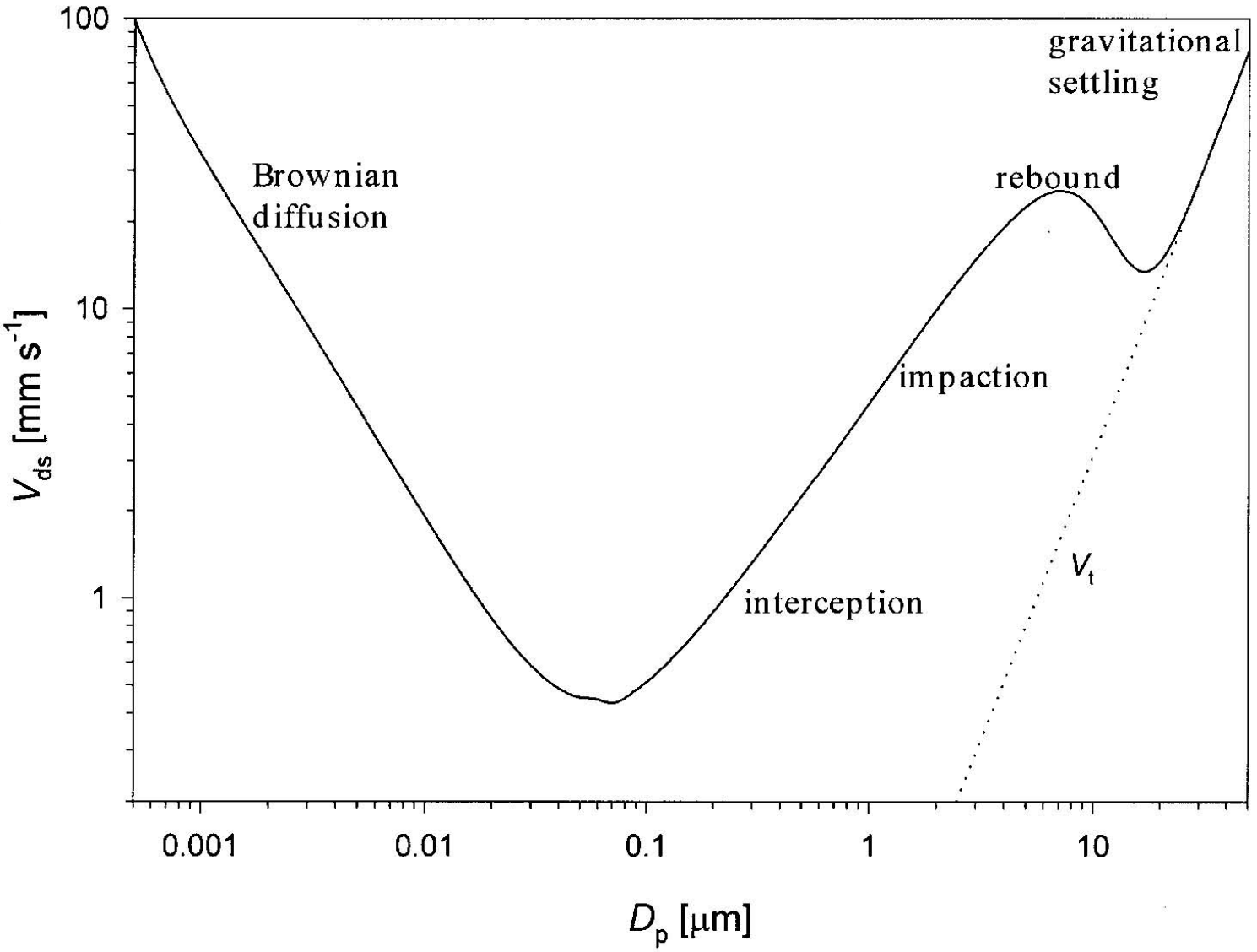

Figure 12.6 The variation with particle diameter of particle surface deposition velocity to a canopy of short (height 0.1 m) vegetation, according to a model proposed by Slinn (1982) (from Fowler et al., 2004). The dominant mechanisms of deposition in each size range are indicated.

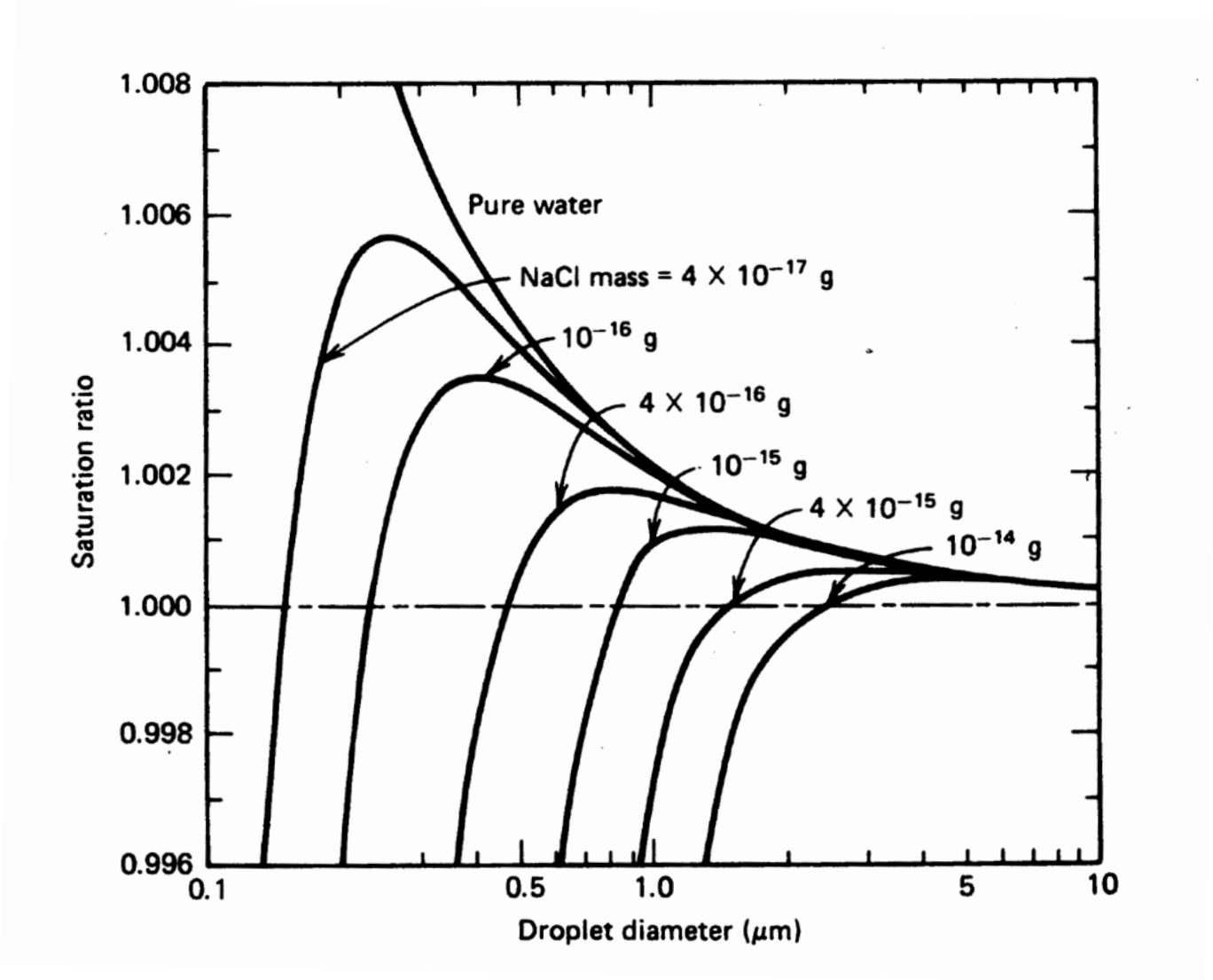

Figure 12.7 Variation of equilibrium droplet diameter with saturation ratio for pure water and for droplets containing the indicated mass of sodium chloride at 20 ◦C (from Hinds, 1999).

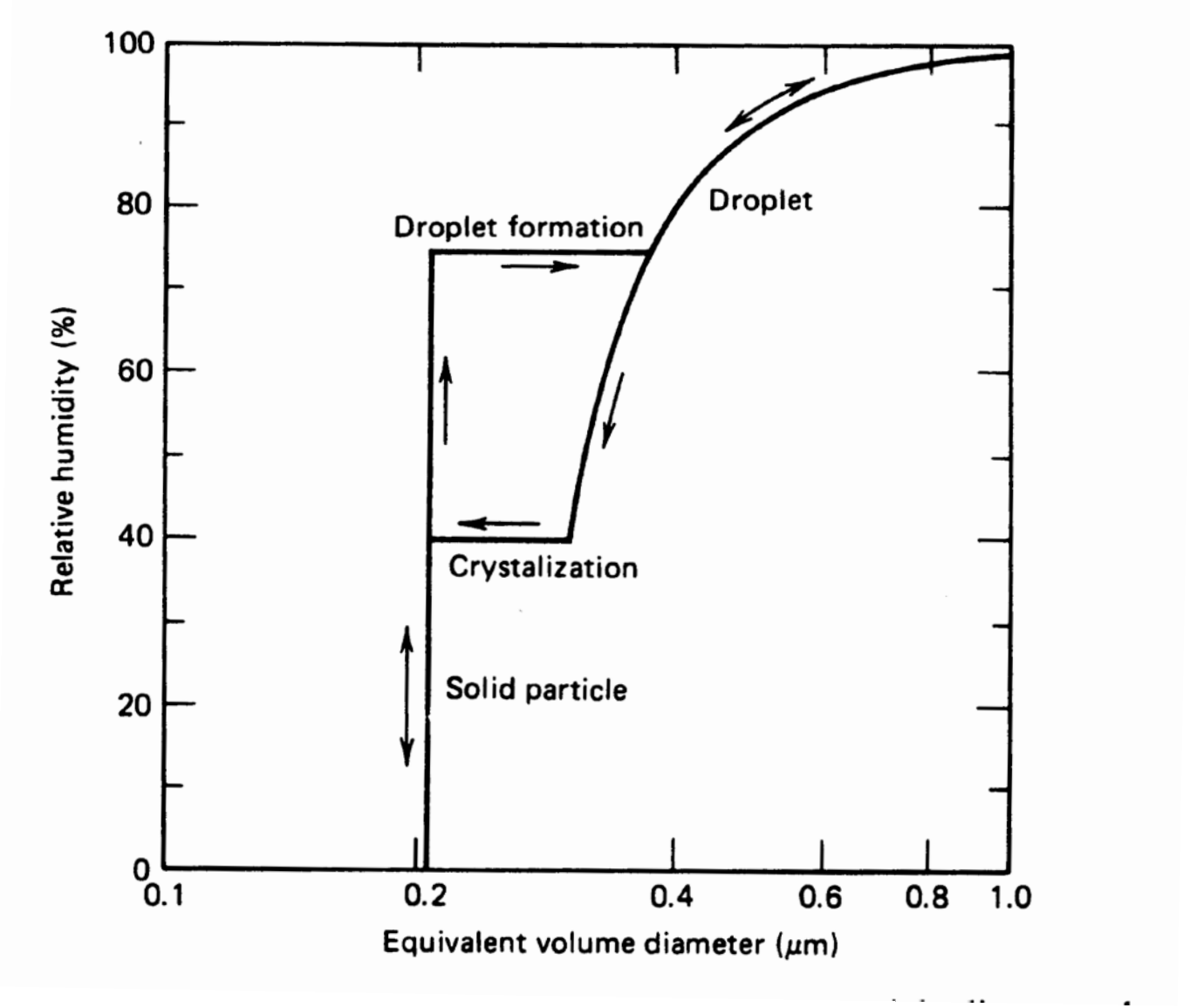

Figure 12.8 The dependence of particle/droplet diameter on relative humidity for a sodium chloride particle of dry mass 10−14 g, showing the transition from a particle to a droplet as humidity increases above 76% and the recrystallization as decreasing humidity reaches 40% (from Hinds, 1999).

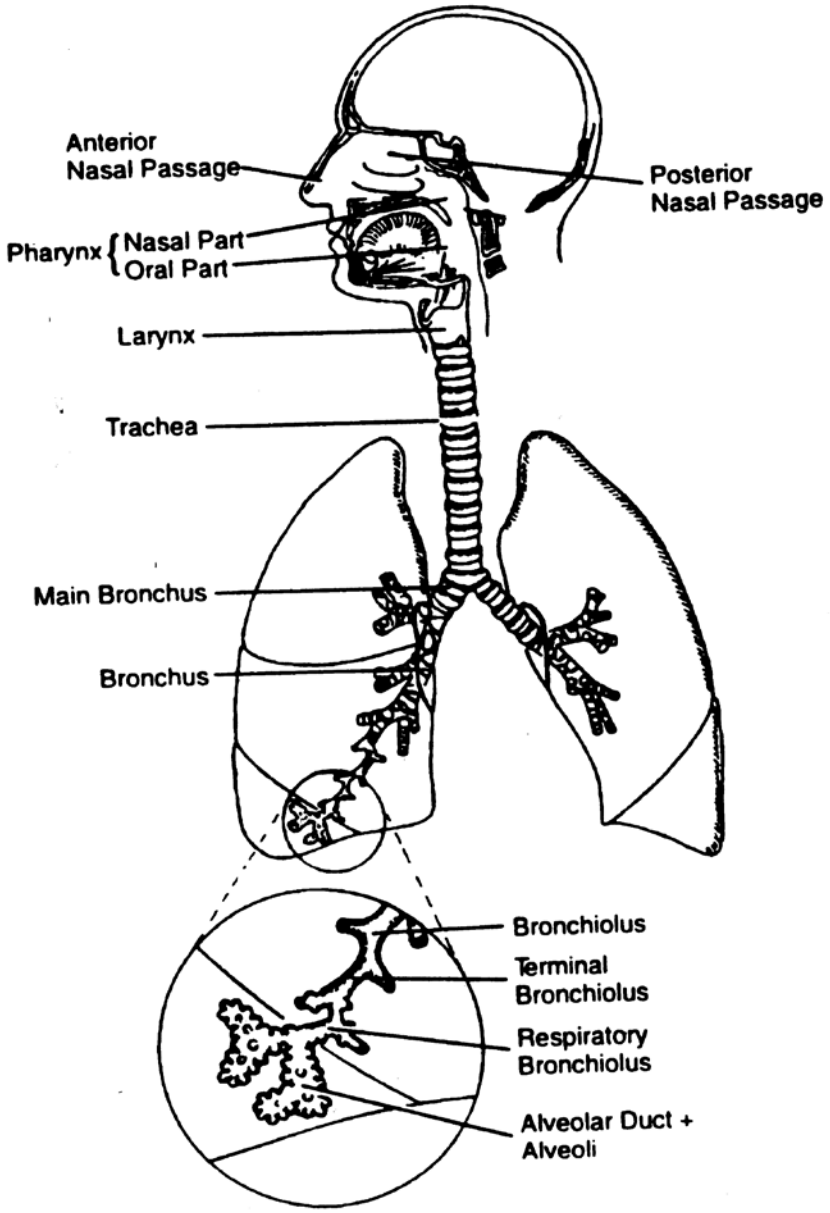

Figure 12.9 The human respiratory system (from Hinds, 1999).

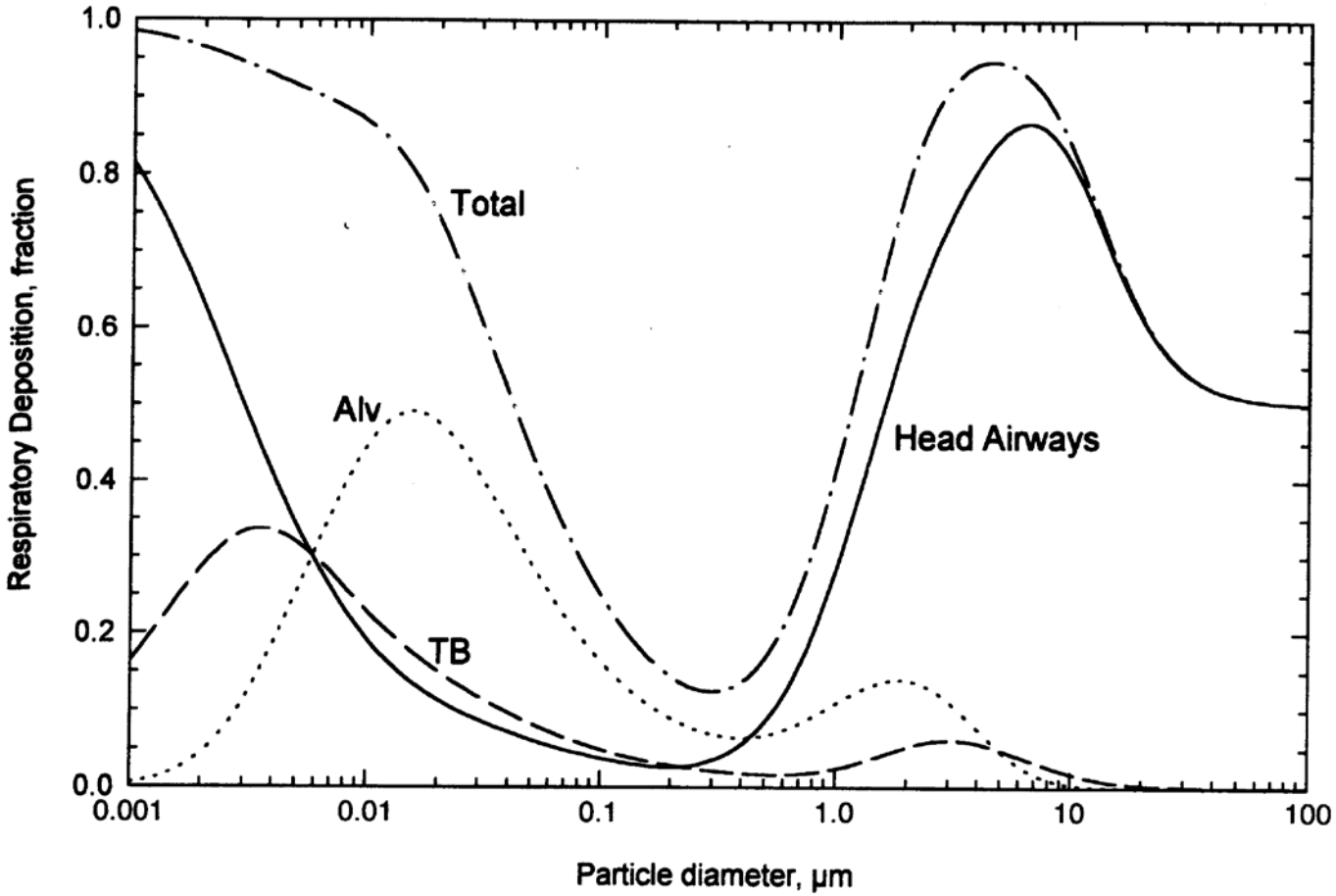

Figure 12.10 Predicted total and regional deposition (Alv -Alveolar airways, TB – Tracheobronchial airways) of aerosol for light exercise (nose breathing) (from Hinds, 1999).